Bioorganic & Medicinal Chemistry 22 (2014) 906–916

Contents lists available at ScienceDirect

Bioorganic & Medicinal Chemistry

journal homepage: www.elsevier.com/locate/bmc

Cholinesterase inhibitory activity versus aromatic core multiplicity: A facile green synthesis and molecular docking study of novel piperidone embedded thiazolopyrimidines

Alireza Basiri [a], Vikneswaran Murugaiyah [a,*], Hasnah Osman [b], Raju Suresh Kumar [c,*], Yalda Kia [b], Alysha Hooda [d], Richard B. Parsons [d]

[a] School of Pharmaceutical Sciences, Universiti Sains Malaysia, Minden 11800, Penang, Malaysia
[b] School of Chemical Sciences, Universiti Sains Malaysia, Minden 11800, Penang, Malaysia
[c] Department of Chemistry, College of Sciences, King Saud University, PO Box 2455, Riyadh, Saudi Arabia
[d] Institute of Pharmaceutical Science, King's College London, London SE1 9NH, UK

ARTICLE INFO

Article history:
Received 10 September 2013
Revised 8 November 2013
Accepted 9 November 2013
Available online 19 November 2013

Keywords:
Domino cascade synthesis
Ionic liquids
Thiazolopyrimidines
AChE and BChE inhibitory activity
Molecular modeling
Aromatic core multiplicity

ABSTRACT

Novel thiazolopyrimidine derivatives have been synthesized via microwave assisted, domino cascade methodology in ionic liquid and evaluated in vitro for their acetylcholinesterase (AChE) and butyrylcholinesterase (BChE) inhibitory activities. Among the newly synthesized compounds **6d**, **6a**, **6e** and **6b** displayed higher AChE inhibitory activity than standard drug, galanthamine, with IC_{50} values of 0.53, 1.47, 1.62 and 2.05 μM, respectively. Interestingly, all the compounds except for **6m–r** and **6x** displayed higher BChE inhibitory potentials than galanthamine with IC_{50} values ranging from 1.09 to 18.56 μM. Molecular docking simulations for **6d** possessing the most potent AChE and BChE inhibitory activities, disclosed its binding interactions at the active site gorge of AChE and BChE enzymes.

1. Introduction

In the context of green chemistry, microwave assisted organic synthesis (MAOS) has gained widespread acceptance in drug discovery laboratories. Those reactions, which are assisted by unrivaled features of ionic liquids such as remarkable catalytic behavior, excellent chemical/thermal stability and good solvating ability, displayed significant merits of reduced reaction time and improved yields.[1,2] Compounds comprising pyrimidine entity were found to exhibit a wide range of biological activities suchlike antitumor,[3–5] anti-inflammatory,[6] adenosine A_{2A} receptor antagonists,[7] antiviral[8,9] as well as potent cholinesterase/Aβ-aggregation inhibitory properties.[10–16] In our pervious study, we reported synthesis and cholinesterase inhibitory activities of novel pyrimidine and thiopyrimidine derivatives, comprising two aromatic rings. These new dual core compounds displayed reasonable cholinesterase inhibitory activities with more selectivity toward BChE.[16]

Alzheimer's disease (AD) is a neurodegenerative disorder that based on the World Health Organization (WHO) report, has affected more than 37 million people worldwide.[17] The etiology of AD is not completely known, however the deposition of extracellular β-amyloid plaques and formation of intracellular neurofibrillary tangles are thought to play principal roles in the pathophysiology of this disease, causing loss of cholinergic neurons in the forebrain, cortex and hippocampus of AD patients.[18–22] The decline in acetylcholine (ACh) neurotransmitter level causes the cognitive impairments seen in AD patients. Thus, increasing ACh levels to restore the cholinergic neurotransmission and improve the cognitive functions in AD patients are of prime importance.[7,23]

Current clinically approved treatments for AD are limited to cholinesterase inhibitors (ChEI's), working by inhibiting cholinesterases from hydrolyzing ACh and *N*-methyl D-aspartate receptor antagonists (e.g. memantine), which act at the glutaminergic pathway.[24–26] Despite the tremendous efforts in search of disease modifying agents working via β-amyloid or tau pathways, none are clinically available due to their adverse effects. Therefore, the search for new cholinesterase enzymes inhibitors is still a promising approach and ongoing worldwide. Two cholinesterases, acetylcholinesterase (AChE) and butyrylcholinesterase (BChE) are responsible for degradation and regulation of ACh in human body, however they differ in kinetics and substrate selectivity.[27] Cholinergic therapy for AD initially focused on AChE inhibition because

* Corresponding authors. Tel./fax: +60 46534583.
E-mail addresses: vicky@usm.my, dr.Murugaiyah@gmail.com (V. Murugaiyah), sraju@ksu.edu.sa (R.S. Kumar).

0968-0896/$ - see front matter © 2013 Elsevier Ltd. All rights reserved.
http://dx.doi.org/10.1016/j.bmc.2013.11.020

Table 1
Residue composition of active sites in *h*AChE and *h*BChE

Entry	Site name	Residue composition in *h*AChE	Residue composition in *h*BChE[38]
1	Catalytic triad	Ser203, His447 and Glu201	His438, Ser198 and Glu325
2	Choline binding site (α-anionic site)	Trp86 and Phe338	Trp82 and Phe329
3	Acyl-binding pocket	Phe295 and Phe297	Leu286 and Val288
4	Oxyanion hole	Gly121, Gly122 and Ala204	Gly116, Gly117 and Ala199
5	Peripheral anionic site (β-anionic site)	Tyr72, Asp74, Tyr124, Trp286, Tyr337 and Tyr341	Trp231, Val288, Leu286 and Phe398

this is the main enzyme involved in the breakdown of ACh in the normal brain.[28] Studies have shown that as the disease progresses, the activity of AChE decreases while the activity of BChE remains unaffected or even increases.[29] Moreover, in the brain of advanced-staged AD patients, BChE can compensate for AChE where the activity of AChE is inhibited and hydrolyze the already depleted levels of ACh.[30,31] Although overall AChE level is reduced in the brain of AD patients, it is increased within and around the amyloid plaques. Since both AChE and BChE hydrolyze ACh and involved in amyloid plaques maturation, inhibition of both enzymes using a dual inhibitor should results in the higher levels of ACh in the brain that provides more significant clinical efficacy.[28] Hence, dual inhibitors are valuable therapeutic compounds in AD therapy.

The active site of human AChE enzyme is located at the bottom of a 20 Å long, narrow gorge comprising five important regions to accommodate and hydrolyze the acetylcholine, namely; catalytic triad,[32] oxyanion hole,[33] choline binding site,[34] acyl binding pocket[35] and peripheral anionic site,[36] (Table 1). Acetylcholine or inhibitors guidance inside the gorge is facilitated by hydrophobic interactions with aromatic amino acid residues lining the gorge wall viz. phenylalanine (Phe), tryptophan (Trp) and tyrosine (Tyr).[37] While the overall structure of human BChE is similar to that of human AChE, the active site of *h*BChE has many of the channel-lining aromatic residues replaced by residues with aliphatic side chains, such as leucine (Leu) and valine (Val), making BChE better able to accommodate bulkier substrates and inhibitors.[38]

Inspired by aforementioned biological significance of dual AChE and BChE inhibitors and in search for new potent Alzheimer's disease modifying agents, in the present study we wish to report ionic liquid mediated synthesis and cholinesterase inhibitory activity study of novel thiazolopyrimidine derivatives comprised of three aromatic rings. Subsequently, the effect of additional aromatic ring on AChE and BChE inhibitory activities and selectivity is compared to dual core inhibitors from our previous report. By the aid of molecular docking studies, the plausible binding interactions mechanisms of the most active derivatives at the active site of AChE and BChE are also explored.

2. Results and discussion

2.1. Chemistry

The highly functionalized α,β-unsaturated ketones (**3**) required for the synthesis of (**6**) were prepared by the Claisen–Schmidt condensation of 4-piperidone hydrochloride (**1**) with a series of aromatic aldehydes in the presence of HCl in acetic acid.[39] The domino cascade reaction of 3,5-diarylidenepiperidin-4-ones (**3**), thiourea (**4**) and α-Bromoacetophenones (**5a–d**) in the ionic liquid, 1-butyl-3-methylimidazolium bromide ([bmim]Br) furnished (*E*)-9-arylidene-3,5-diaryl-6,7,8,9-tetrahydro-5*H*-pyrido[4,3-*d*]thiazolo[3,2-*a*]pyrimidines (**6a–x**) in good yield. (Scheme 1)

In order to find an optimal and efficient protocol for the synthesis of **6**(**a–x**), we initiated our study by performing the model reaction of an equimolar ratio of *para*-methyl derivative of 3,5-bis-(aryledene)piperidin-4-one (**3**), thiourea (**4**) and 2-bromo-4′-chloroacetophenone (**5b**), employing two different synthetic approaches. In the first approach, the synthetic potential of a one pot, three component reaction was investigated using one molar equivalent of ([bmim]Br). Owing to the slow reaction rate of 3,5-bis-(aryledene)piperidin-4-one (**3**) with thiourea (**4**), in contrast to the relatively fast reaction of (**4**) and (**5**), this methodology failed to furnish the proposed thiazolopyrimidines (**6**).

Thus, we carried out a domino cascade two-step reaction by refluxing 3,5-bis-(aryledene)piperidin-4-one (**3**) and thiourea (**4**) in 1 molar equivalent of [bmim]Br for 2 h, as the first step. In the second step, 2-bromo-4′-chloroacetophenone (**5b**) were added to

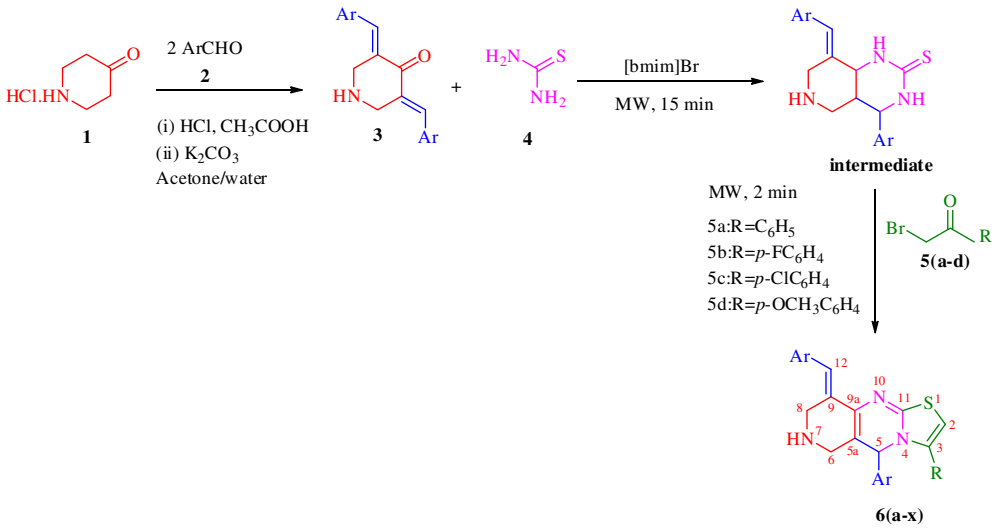

Scheme 1. Synthesis of **6**(**a–x**).

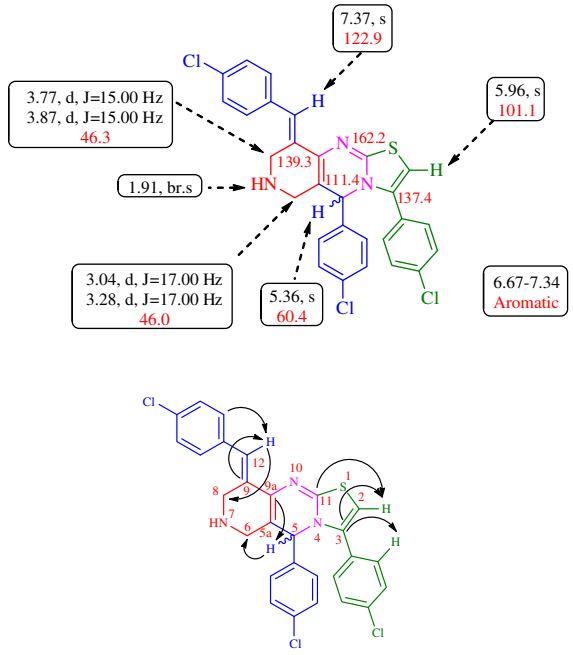

Figure 1. Selected HMBCs and ^{1}H and ^{13}C chemical shifts of **6q**.

mixture without isolating the intermediates and reaction continued for additional 2 h. After completion of the reaction as evident by TLC, the thiazolopyrimidine product was isolated in moderate yield through column chromatography (57%). Consequently, the same reaction was investigated under microwave irradiation as a valuable alternative for conventional heating. As expected, the first step of the reaction was completed in less than 15 min followed by the next step, which interestingly was completed in less than 2 min.

The domino cascade methodology reinforced by the unique properties of ionic liquid and features of microwave irradiation method enabled us to furnish a library of hitherto unreported thiazolopyrimidines rapidly and in good yield. The selection of different aldehydes and 2-bromo-acetophenones is based on the fact that these groups consist of a wide range of electron donating and electron withdrawing moieties enabling us to investigate their inhibitory effects on the AChE and BChE enzymes. On the other hand, derivatives such as chloro, fluoro and methoxy showed positive influence on the inhibitory activities of synthesized compounds in our previous study.[16]

Structural elucidation of the thiazolopyrimidines (**6a–x**) was accomplished using 1D and 2D NMR spectroscopy techniques as well as elemental analysis. In the ^{1}H NMR spectrum of **6q**, the one hydrogen singlet at 5.36 ppm is due to H-5 and from HMQC the peak at 60.4 ppm was assigned to C-5. Further, H-5 shows HMBCs with C-6 at 46.0 ppm besides showing correlation with C-5a and C-11 at 114.4 and 162.0 ppm, respectively. From HMQC, the doublets at 3.04 and 3.28 ppm (J = 17.00 Hz) was assigned to H-6a and H-6b whilst the other doublets at 3.77 and 3.87 ppm (J = 15.00 Hz) can be attributed to H-8a and H-8b. The singlets at 7.37 ppm and 5.96 ppm are due to H-12 and H-2, the later shows HMBCs with C-3 at 137.4 ppm. The multiplets around 6.67–7.34 ppm is due to aromatic hydrogens. These assignments are also supported by the HMBC. The ^{1}H and ^{13}C chemical shifts as well as HMBC correlations of **6q** are depicted in Figure 1.

A plausible mechanism for the formation of (**6**) in the presence of ([bmim]Br) is described in Scheme 2. As ([bmim]Br) plays dual role as both solvent and catalyst, it facilitates the reaction by forming H-bond between the electron deficient hydrogen atom of ionic liquid with the oxygen atom of carbonyl functionality in **3**. Initial Michael addition of thiourea to β position of α,β-unsaturated ketone followed by sequential condensation/tautomerization affords the intermediate A. In the next step, a five membered thiazoline ring formed via tautomerization of NH–C=S bond to negatively charged sulfur atom and its subsequent nucleophilic addition to positively charged carbon atom of CH_2–Br bond in 2-bromoacetophenones and eventually nucleophilic addition and elimination of secondary amine to carbonyl moiety via enamine pathway as depicted in scheme 2.

2.2. In vitro cholinesterase enzymes inhibitory activities

All the newly synthesized compounds were evaluated for their cholinesterases inhibitory activities against AChE derived from *Electrophorus electricus* and BChE from equine serum. The active sites of cholinesterase enzymes establish extensive hydrophobic interactions with their inhibitors/substrates owing to high aromatic content. In the present study, we aimed to evaluate a variety of thiazolopyrimidines derivatives comprising three aromatic cores to investigate how aromatic content and multiplicity affect AChE/BChE inhibitors potencies.

The molecular structure of **6** is composed of three distinctive regions, namely: R; comprising phenyl, *p*-fluoro phenyl, *p*-chloro phenyl and *p*-methoxy phenyl moieties, Ar; ascribing versatile phenyl derivatives, which both are engrafted to an aliphatic thiazolopyrimidine core.

AChE inhibitory activities of thiazolopyrimidine derivatives are summarized in Table 2. Compounds **6a–f**, bearing un-substituted

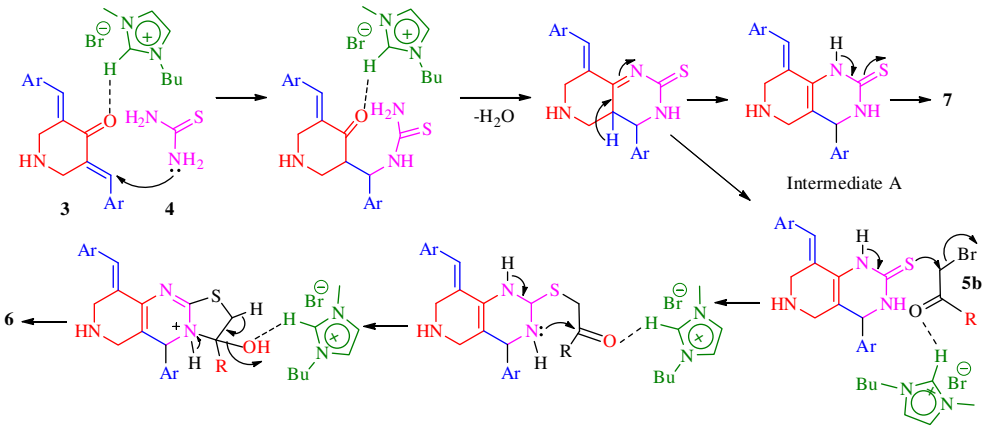

Scheme 2. Plausible mechanism for the formation of **6**.

Table 2
Physical data, AChE and BChE inhibitory activities of **6(a–x)**

Entry	Compound	R	Ar	Yield (%)	AChE inhibition (IC_{50})		BChE inhibition (IC_{50})		Selectivity	
					(μg/ml)	(μM)	(μg/ml)	(μM)	AChE[a]	BChE[b]
1	6a	C_6H_5	C_6H_5	86	0.6 ± 0.04	1.47	0.70 ± 0.03	1.74	1.19	0.84
2	6b		*o*-ClC_6H_4	79	1.03 ± 0.11	2.05	1.34 ± 0.07	2.68	1.30	0.77
3	6c		*o*-(OCH3)C_6H_4	82	2.08 ± 0.15	4.23	2.02 ± 0.11	4.10	0.97	1.03
4	6d		*p*-$CH_3C_6H_4$	84	0.24 ± 0.02	0.53	0.79 ± 0.04	1.71	3.21	0.31
5	6e		*p*-ClC_6H_4	81	0.81 ± 0.05	1.62	1.09 ± 0.08	2.18	1.35	0.74
6	6f		*p*-FC_6H_4	85	1.89 ± 0.09	4.04	1.85 ± 0.12	3.95	0.98	1.02
7	6g	*p*-FC_6H_4	C_6H_5	81	9.17 ± 0.15	20.32	3.57 ± 0.14	7.91	0.39	2.57
8	6h		*o*-ClC_6H_4	73	3.14 ± 0.11	6.03	2.41 ± 0.08	4.63	1.30	0.76
9	6i		*o*-(OCH3)C_6H_4	75	2.81 ± 0.09	5.50	4.47 ± 0.19	8.75	1.59	0.63
10	6j		*p*-$CH_3C_6H_4$	79	3.10 ± 0.18	6.47	2.35 ± 0.17	4.91	0.76	1.32
11	6k		*p*-ClC_6H_4	71	2.98 ± 0.12	5.73	8.21 ± 0.22	15.80	2.75	0.36
12	6l		*p*-FC_6H_4	68	6.41 ± 0.22	13.16	7.68 ± 0.25	15.77	1.20	0.83
13	6m	*p*-ClC_6H_4	C_6H_5	79	11.16 ± 0.11	23.85	20.75 ± 0.22	44.34	1.86	0.54
14	6n		*o*-ClC_6H_4	82	2.78 ± 0.05	5.20	4.10 ± 0.16	7.65	1.47	0.68
15	6o		*o*-(OCH3)C_6H_4	81	2.68 ± 0.07	5.08	15.45 ± 0.27	29.28	5.76	0.17
16	6p		*p*-$CH_3C_6H_4$	83	10.78 ± 0.15	21.74	16.14 ± 0.17	32.56	1.50	0.67
17	6q		*p*-ClC_6H_4	85	2.87 ± 0.10	5.37	14.70 ± 0.18	27.43	5.11	0.20
18	6r		*p*-FC_6H_4	78	5.16 ± 0.11	10.27	11.18 ± 0.20	22.24	2.16	0.46
19	6s	*p*-$(OCH_3)C_6H_4$	C_6H_5	80	7.36 ± 0.14	15.92	4.82 ± 0.17	10.41	0.65	1.52
20	6t		*o*-ClC_6H_4	76	4.24 ± 0.12	7.97	6.68 ± 0.25	12.56	1.58	0.63
21	6u		*o*-(OCH3)C_6H_4	79	6.26 ± 0.21	11.97	9.7 ± 0.22	18.56	1.55	0.64
22	6v		*p*-$CH_3C_6H_4$	84	4.90 ± 0.10	10.44	5.14 ± 0.18	10.48	1.01	0.99
23	6w		*p*-ClC_6H_4	87	4.49 ± 0.17	8.44	6.81 ± 0.19	12.79	1.52	0.66
24	6x		*p*-FC_6H_4	83	11.18 ± 0.19	22.41	13.25 ± 0.24	26.55	1.18	0.84
25		Galanthamine			0.60 ± 0.01	2.09	5.55 ± 0.01	19.34	3.47	0.28

[a] Selectivity for AChE is defined as IC_{50}(BChE)/IC_{50}(AChE).
[b] Selectivity for BChE is defined as IC_{50}(AChE)/IC_{50}(BChE).

phenyl moiety in region 'R', displayed highest inhibitory activities with IC_{50} values of lower than 4.5 μM. Therein, compound **6d** with (Ar = *p*-methylphenyl), showed highest AChE inhibitory activity with sub-micromolar IC_{50} value of 0.53 μM, which is four times higher than standard drug, galanthamine with IC_{50} value of 2.09 μM.

Structure activity relationship (SAR) study for compounds **6a–x** clearly showed that substitution on region 'R' is a major determinant of AChE inhibitory activity. In addition, the planar configuration of thiazolopyrimidine compounds provides less hindered insertion and better accommodation inside the narrow AChE active site channel. Moreover, the polarizable sulfur atom of thiazoline ring and free nitrogen atom of piperidone ring effectively interact with electron rich aromatic gorge of AChE through mild polar (dipole–induced dipole) interactions. 'Dipole–induced dipole' interactions, mostly occurs between a permanent dipole such as C═O, C–S or C–N and molecules with π electrons, like benzene rings of phenylalanine and tyrosine.

Moving from **6a–f** with (R = phenyl) to **6g–l** with (R = *p*-fluorophenyl) then **6m–r** with (R = *p*-chlorophenyl) and finally **6s–x** with (R = *p*-methoxyphenyl), a decline in AChE inhibitory activities is observed. This is presumably due to the enlargement of 'R' that led to more hindered insertion and improper accommodation of inhibitors inside the active site channel of the AChE enzyme.

On the other hand, substitution on region 'Ar' showed only a minor effect on the AChE inhibition of these derivatives. However, the presence of a chloro atom on either *ortho* or *para* position of the phenyl ring of 'Ar' improved the inhibitory potencies, with IC_{50} values ranging from 1.62 to 8.44 μM. In addition, compounds **6i** and **6o** with Ar = *o*-methoxyphenyl and **6j** with Ar = *p*-methylphenyl also displayed good inhibitory activities with IC_{50} values of lower than 10 μM.

Regarding BChE inhibitory activities, compounds **6a–j** and **6n** displayed remarkable potencies with IC_{50} values of lower than

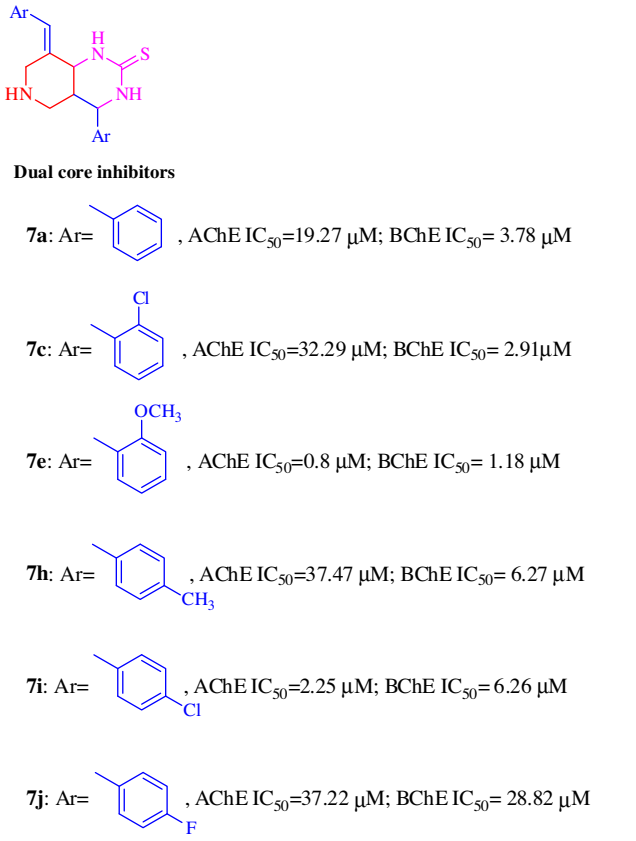

Figure 2. Schematic representation of dual core inhibitors, their derivatives, AChE and BChE inhibitory activities.

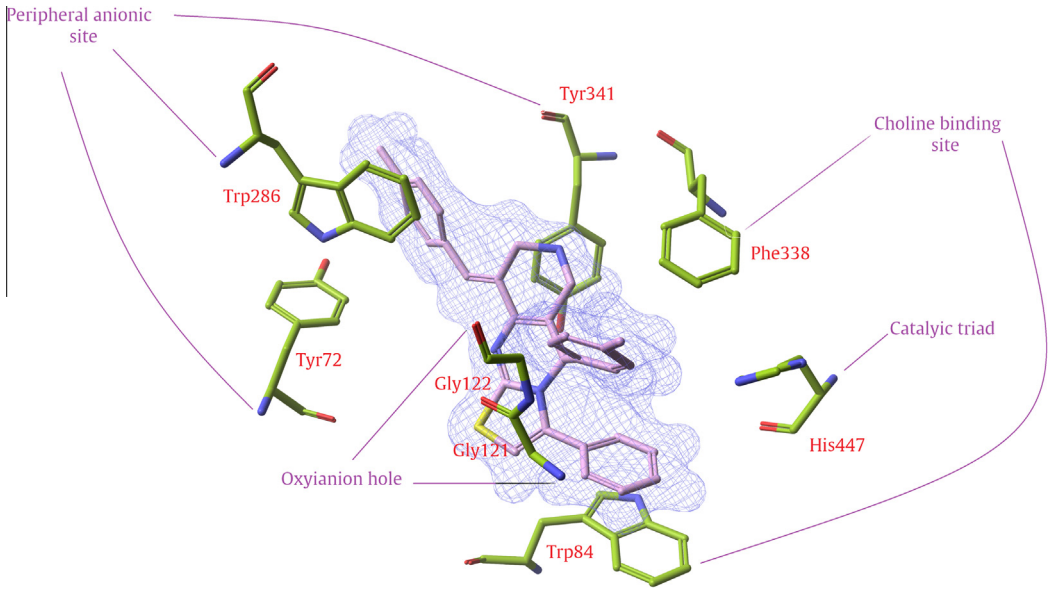

Figure 3. Binding interaction of **6d** with major active site residues of *h*AChE.

9 μM, therein compound **6d** displayed highest activity with IC_{50} value of 1.71 μM, almost 10 times stronger than the standard drug. Rest of the compounds displayed moderate activities with IC_{50} values ranging from 10.41 to 44.34 μM. The effect of 'R-substitution' on BChE inhibitory activities was similar to AChE except for compounds **6m–r** with R = *p*-methoxyphenyl which displayed better activities than **6g–l** with R = *p*-chlorophenyl. This effect is probably due to the larger active site of BChE enzyme, which preferably accommodates more energetically favorable inhibitors irrespective to their size.

In our previous study, we reported synthesis and cholinesterase inhibitory activities of novel pyridopyrimidothione derivatives comprising two aromatic rings.[16] To get better insight into the effect of aromaticity on cholinesterase inhibitory activities, compounds **6a–x** composed of three aromatic cores compared to their dual core analogs possessing similar substituent on phenyl ring of 'Ar', viz. **7a**, (Ar = phenyl, IC_{50} = 19.27); **7c**, (Ar = *o*-chlorophenyl, IC_{50} = 32.39); **7e**, (Ar = *o*-methoxyohenyl, IC_{50} = 0.8); **7h**, (Ar = *p*-methylphenyl, IC_{50} = 37.47); **7i**, (Ar = *p*-chlorophenyl, IC_{50} = 2.25) and **7j**, (Ar = *p*-fluorophenyl, IC_{50} = 37.22 μM) (Fig. 2). The results indicated that, except for compounds **6c** and **6i**, the rest of triple core thiazolopyrimidines in this study displayed 1.5 to 70 fold higher AChE inhibitory activities than their dual core analogs. Compounds **6a–f** ascribing phenyl as the additional aromatic moiety in 'R', represented highest variation in the activities observed, therein compound **6d** displayed almost 70 times higher AChE inhibitory activity than dual core **7h** (IC_{50} = 0.53 vs 37.47 μM).

This phenomenon is presumably due to the high aromatic content of AChE enzyme active site enabling it to establish strong hydrophobic and π,π-stacking interactions with the substrate or inhibitors, employing its aromatic amino acid residues. So, the inhibitors with three aromatic cores were found to interact more

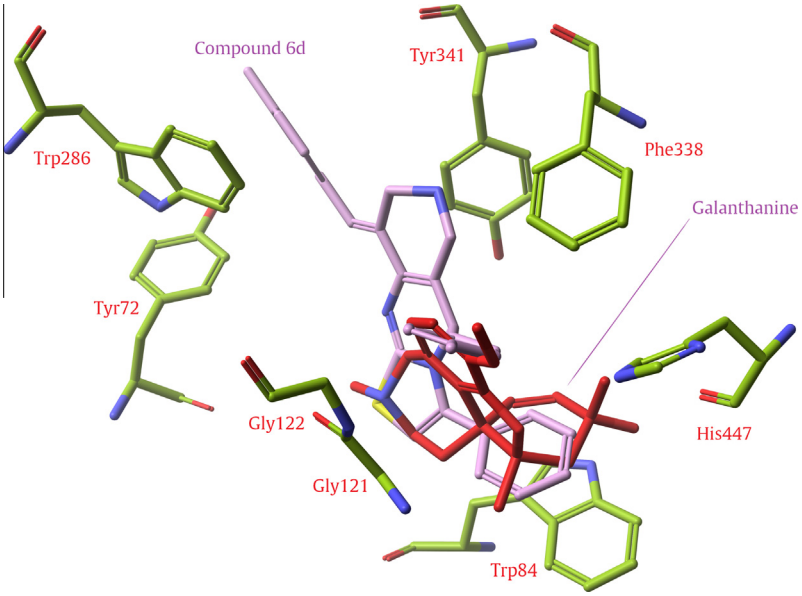

Figure 4. Orientation of **6d** superimposed with galanthamine in active site of *h*AChE enzyme.

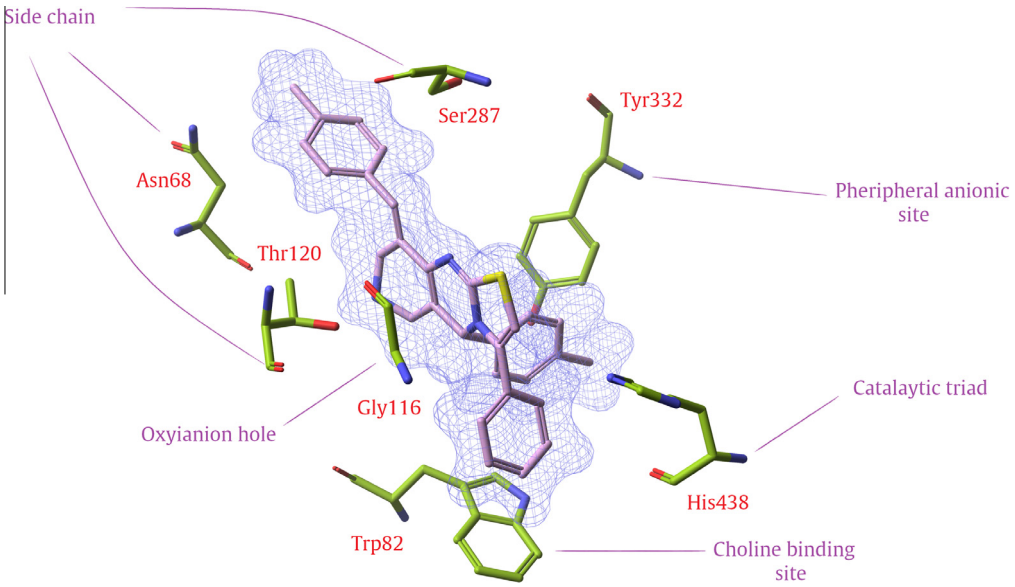

Figure 5. Binding interaction of **6d** with major active site residues of *h*BChE.

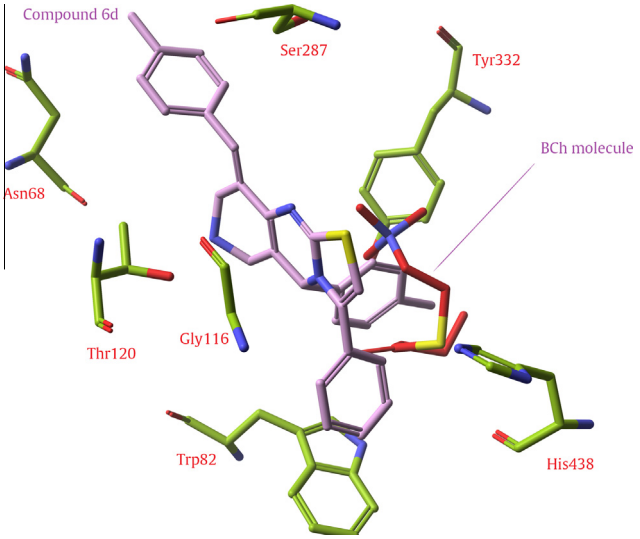

Figure 6. Orientation of **6d** superimposed with BCh molecule in active site of *h*BChE enzyme.

efficiently with the AChE channel wall, facilitating their insertion and accommodation into the gorge. However, the size of the additional aromatic core has to be chosen wisely due to constriction of AChE gorge. As in our case, compounds **6a–f** bearing relatively small phenyl moiety as third aromatic core, displayed highest inhibitory activity in contrast to larger 'R' substituents viz. fluoro, chloro and methoxy phenyl.

Unlike AChE, for BChE most of the triple core thiazolopyrimidines displayed lower activity than their dual core analogs namely; **7a**, **7c**, **7e**, **7h**, **7i**, and **7j** having IC_{50} values of 3.78, 2.91, 1.18, 6.27, 6.26 and 28.82 μM, respectively. As mentioned earlier, in the active site of BChE, aromatic residues such as tyrosine and tryptophan are mostly replaced with hydrophobic valine and leucine residues. These changes reduces BChE active site ability to form hyrdophobic and π,π-stacking interactions with aromatic cores comparing to AChE. Although, engraftment of new aromatic core slightly increased the activities for **6a**, **6b**, **6d**, **6e**, **6f**, **6i** and **6l**, but it considerably decreased activities for the remaining compounds comparing to their dual core analogs.

It is also worth to mention that expect for compounds **6g**, **6j** and **6s**, which showed more selectivity toward BChE, all the newly synthesized thiazolopyrimidines had more selectivity for AChE. In addition, compounds **6a–f** except **6d** displayed potent dual inhibitory properties. AChE specific inhibitors might be useful at the earlier stages of AD whereby AChE enzyme has dominant role in breaking down the ACh. However, as the disease progresses, BChE role become more prominent and therefore a dual inhibitor is expected to be beneficial at both stage.

2.3. Molecular docking studies

Molecular docking simulations were performed on compounds **6d** that displayed the highest AChE and BChE inhibitory activities among the compounds **6a–x** to gain functional and structural insight into its binding interaction at the active sites of human AChE and BChE enzymes.

These molecular docking analysis for **6d** disclosed that the majority of its binding interactions with *h*AChE receptor were mild polar and hydrophobic in nature. As mentioned before, mild polar interaction can be defined as the 'dipole–induced dipole interactions' which mostly occurs between a permanent dipole and molecules with π electrons, such as phenylalanine and tyrosine. The 'Ar' moieties of this compound viz. *p*-methylphenyl, displayed relatively strong π,π-stacking interaction with aromatic rings of Tyr72 and Tyr341 at peripheral anionic as well as Phe338 at choline binding site of the enzyme located at the entrance of the gorge. Besides, the phenyl group of 'R', also established a π,π-stacking interaction with another choline binding site residue, Trp84, at the bottom of the gorge. Hydrophobic interactions with Phe295 and Phe297 at acyl binding pocket as well as mild polar interactions with Gly121 and Gly122 at oxyanion hole and His447, Ser203 at catalytic triad are the other dominant interactions of **6d** with the active site residues of *h*AChE receptor (Fig. 3). This binding template including all the five main sub-sites of AChE receptor obviously coincided with significant inhibitory activity of **6d** contrasting to standard drug. Crystal structure of AChE in complex with available Alzheimer's drug galanthamine, also showed similar template of occupying the peripheral anionic site,

Table 3
Binding interaction data for **6d** docked into active site gorge of *h*AChE and *h*BChE receptors

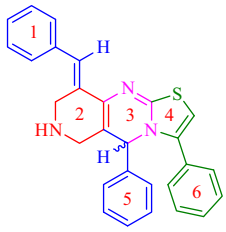

Entry	Ligand	Enzyme	Docking score	Interacting site	Amino acid residue	Bond type	Ligand interacting moiety
1	**6d**	*h*AChE	−9.2	PAS[a]	Trp286	Hydrophobic	Ring 1
					Tyr72	π–π stacking	
					Tyr341	Hydrophobic	Ring 2
					Tyr124	Hydrophobic	
				OH[b]	Gly121 and 122	Mild polar	Ring 4
					Ala204	Hydrophobic	
				Acyl binding pocket	Phe295	Hydrophobic	
					Phe297	Hydrophobic	
				Choline binding site	Phe338	π–π Stacking	
					Trp86	π–π Stacking	Ring 6
				CT[c]	Ser203	Mild polar	Ring 4
					His447	Mild polar	
2	**6d**	*h*BChE	−7.7	Side chain	Asn68	Mild polar	Ring 1
					Ser287	Mild polar	
					Thr120	H-bonding	Ring 2, NH
				PAS	Leu286	Hydrophobic	Ring 5
				OH	Gly116 and 117	Mild polar	
				Choline binding site	Phe329	Hydrophobic	Ring 6
					Trp82	π–π Stacking	Ring 4
				CT	His438	π–π Stacking	Ring 6
					Ser198	Mild polar	Ring 5

[a] Peripheral anionic site.
[b] Oxyanion hole.
[c] Catalytic triad.

stacking against Trp86 and interaction with residues at catalytic triad (Fig. 4).[40]

Regarding molecular docking simulation on BChE receptor, aromatic cores of 'R' and 'Ar' in **6d** displayed effective π,π-stacking interaction with His438 in the catalytic triad and Trp82 at the choline binding site of BChE enzyme, along with H-bonding interaction with the side chain hydroxyl of Thr120. This binding orientation, in addition to the mild polar interaction with oxyanion hole residues Gly116 and Gly117 as well as catalytic triad residue Ser198 confirmed the complete insertion and efficient accommodation of this inhibitor inside the active site gorge of the BChE receptor (Fig. 5). Moreover, the crystal structure of BChE enzyme in complex with its substrate, butrylylcholine, also showed the similar interaction pattern of occupying choline binding site and stacking against Trp82 as well as interaction with the residues composing catalytic triad of the enzyme (Fig. 6).

The data representing free binding energies, receptor interaction sites, ligand interacting moieties, amino acid residues involved in ligand–receptor complex as well as bonding types of compound **6d** are summarized in Table 3.

3. Conclusion

A library of hitherto unreported pyrimidine grafted heterocycles comprising three aromatic cores were synthesized via an efficient methodology in ionic liquid [bmim]Br, with good yields and investigated to disclose the effect of aromatic core multiplicity on cholinesterases inhibition. In vitro cholinesterase inhibitory results revealed that engraftment of the third aromatic core significantly improved AChE inhibitory activities up to 70 fold. However, this phenomenon was inversely correlated to the size of embedded aromatic entity, due to constriction of AChE gorge and its sensivity to the size of inhibitors. In general, triple core inhibitors in the present study displayed better inhibition and selectivity toward AChE in comparison to dual core ones, which mostly displayed better selectivity for BChE. However, addition of un-substituted phenyl moiety as the third aromatic core significantly increased both AChE and BChE inhibitory activities in contrast to their previously reported dual core analogs.

4. Experimental

4.1. Chemistry

Melting points were recorded using Stuart Scientific (SMP1) apparatus and are uncorrected. A CEM microwave synthesizer (Model: Discover-S908860) operating at 180/240 V and 50/60 Hz with consumption of 1100 W with microwave power maximum level of 300 W and microwave frequency of 2455 MHz was employed for the irradiation done in this work. The ^{1}H, ^{13}C and the 2D NMR spectra were recorded on a Bruker (Avance) 500 MHz NMR instrument using TMS as internal standard and $CDCl_3$ as solvent. Bruker Topspin 3.0 software was used to process the NMR data. Chemical shifts are given in parts per million (δ-scale) and the coupling constants are given in Hertz. Silica gel-G plates (Merck) were used for TLC analysis with a mixture of petroleum ether (60–80 °C) and ethyl acetate as eluent. Elemental analyses were accomplished on a Perkin Elmer 2400 Series II Elemental CHN analyzer.

4.1.1. General procedure for the synthesis of compounds (6a–x)

An equimolar mixture of (3*E*,5*E*)-3,5-bis-arylidene-piperidin-4-one (**3**) and thiourea (**4**) were allowed to react under microwave

irradiation (100 °C) by using 1 molar equivalent of [bmim]Br as ionic liquid. After 15 min 2-bromoacetophenones (**5a**–**d**) were added to the mixture without isolating the intermediate and reaction continued for another 2 min. After completion of the reaction as evident by TLC, the products (**6a**–**x**) were isolated in good yields via purification by column chromatography using 7.5:2.5 petroleum ether/ethyl acetate solvent system.

4.1.1.1. (*E*)-9-Benzylidene-3,5-diphenyl-6,7,8,9-tetrahydro-5*H*-pyrido[4,3-*d*]thiazolo[3,2-*a*]pyrimidine (6a). Yellow solid; yield: 86%, mp 216–219 °C; Anal. Calcd for $C_{28}H_{23}N_3S$: C, 77.57; H, 5.35; N, 9.69; Found: C, 76.17; H, 5.25; N, 9.55; ^{1}H NMR (500 MHz, $CDCl_3$): δ_H 2.04 (br s, 1H, NH), 3.01 (d, J = 17.20 Hz, 1H, H-6a), 3.22 (d, J = 17.20 Hz, 1H, H-6b), 3.75 (d, J = 15.00 Hz, 1H, H-8a), 3.92 (d, J = 15.00 Hz, 1H, H-6b), 5.39 (s, 1H, H-5), 5.89 (s, 1H, H-2), 6.55–7.39 (m, 15H, H-aromatic), 7.41 (s, 1H, H-12). ^{13}C NMR (125 MHz, $CDCl_3$): δ_C 45.61, 45.79, 60.69, 100.11, 110.38, 124.51, 126.34, 128.39, 128.74, 128.95, 129.03, 129.18, 129.28, 130.32, 130.54, 134.09, 134.31, 136.41, 137.97, 138.21, 139.08, 162.57.

4.1.1.2. (*E*)-9-(2-Chlorobenzylidene)-5-(2-chlorophenyl)-3-phenyl-6,7,8,9-tetrahydro-5*H*-pyrido[4,3-*d*]thiazolo[3,2-*a*]pyrimidine (6b). Yellow solid; yield: 79%, mp 162–165 °C; Anal. Calcd for $C_{28}H_{21}Cl_2N_3S$: C, 66.93; H, 4.21; N, 8.36; Found: C, 66.88; H, 4.19; N, 8.27; ^{1}H NMR (500 MHz, $CDCl_3$): δ_H 2.04 (br s, 1H, NH), 3.04 (d, J = 17.27 Hz, 1H, H-6a), 3.30 (d, J = 17.27 Hz, 1H, H-6b), 3.77 (d, J = 15.48 Hz, 1H, H-8a), 3.89 (d, J = 15.48 Hz, 1H, H-8b), 5.44 (s, 1H, H-5), 5.96 (s, 1H, H-2), 6.55–7.41 (m, 13H, H-aromatic), 7.43 (s, 1H, H-12). ^{13}C NMR (125 MHz, $CDCl_3$): δ_C 46.29, 46.58, 60.65, 100.71, 111.39, 123.17, 128.10, 128.55, 128.65, 128.93, 129.02, 129.44, 130.50, 130.72, 132.51, 132.72, 134.68, 136.10, 139.07, 139.75, 162.71.

4.1.1.3. (*E*)-9-(2-Methoxybenzylidene)-5-(2-methoxyphenyl)-3-phenyl-6,7,8,9-tetrahydro-5*H*-pyrido[4,3-*d*]thiazolo[3,2-*a*]pyrimidine (6c). Yellow solid; yield: 82%, mp 172–174 °C; Anal. Calcd for $C_{30}H_{27}N_3O_2S$: C, 73.00; H, 5.51; N, 8.51; Found: C, 73.07; H, 5.59; N, 8.54; ^{1}H NMR (500 MHz, $CDCl_3$): δ_H 2.86 (d, J = 16.55 Hz, 1H, H-6a), 3.42 (d, J = 16.55 Hz, 1H, H-6b), 3.62 (s, 3H, methoxy), 3.80 (s, 1H, methoxy), 3.82-3.89 (m, 2H, H-8), 5.41 (s, 1H, H-5), 5.96 (s, 1H, H-2), 6.48-7.75 (m, 14H, H-aromatic, H-12). ^{13}C NMR (125 MHz, $CDCl_3$): δ_C 52.41, 53.38, 55.07, 55.24, 60.57, 100.57, 108.18, 125.11, 127.72, 127.89, 128.41, 128.62, 128.82, 129.11, 130.66, 133.15, 135.75, 139.11, 162.37.

4.1.1.4. (*E*)-9-(4-Methylbenzylidene)-3-phenyl-5-*p*-tolyl-6,7,8,9-tetrahydro-5*H*-pyrido[4,3-*d*]thiazolo[3,2-*a*]pyrimidine (6d). Yellow solid; yield: 84%, mp 140–142 °C; Anal. Calcd for $C_{30}H_{27}N_3S$: C, 78.06; H, 5.90; N, 9.10; Found: C, 78.16; H, 5.95; N, 9.17; ^{1}H NMR (500 MHz, $CDCl_3$): δ_H 2.22 (s, 3H, CH_3), 2.33 (s, 3H, CH_3), 2.56 (br s, 1H, NH), 3.07 (d, J = 17.25 Hz, 1H, H-6a), 3.28 (d, J = 17.25 Hz, 1H, H-6b), 3.80 (d, J = 15.10 Hz, 1H, H-8a), 3.97 (d, J = 15.10 Hz, H-8b), 5.41 (s, 1H, H-5), 5.92 (s, 1H, H-2), 6.55–7.39 (m, 13H, H-aromatic), 7.45 (s, 1H, H-12). ^{13}C NMR (125 MHz, $CDCl_3$): δ_C 45.62, 45.82, 60.72, 100.13, 110.40, 124.50, 126.34, 128.37, 128.75, 128.92, 129.04, 129.20, 129.27, 130.33, 130.60, 134.13, 134.34, 136.45, 137.99, 138.17, 139.02, 162.54.

4.1.1.5. (*E*)-9-(4-Chlorobenzylidene)-5-(4-chlorophenyl)-3-phenyl-6,7,8,9-tetrahydro-5*H*-pyrido[4,3-*d*]thiazolo[3,2-*a*]pyrimidine (6e). Yellow solid; yield: 81%, mp 165–167 °C; Anal. Calcd for $C_{28}H_{21}Cl_2N_3S$: C, 66.93; H, 4.21; N, 8.36; Found: C, 66.82; H, 4.27; N, 8.44; ^{1}H NMR (500 MHz, $CDCl_3$): δ_H 2.06 (br s, 1H, NH), 3.06 (d, J = 17.37 Hz, 1H, H-6a), 3.31 (d, J = 17.37 Hz, 1H, H-6b), 3.79 (d, J = 15.48 Hz, 1H, H-8a), 3.92 (d, J = 15.48 Hz, 1H, H-8b), 5.46 (s, 1H, H-5), 5.99 (s, 1H, H-2), 6.62–7.45 (m, 14H, H-aromatic, H-12). ^{13}C NMR (125 MHz, $CDCl_3$): δ_C 46.32, 46.60, 60.71, 100.83, 111.60, 123.37, 128.20, 128.71, 128.93, 129.09, 129.16, 129.65, 130.70, 130.96, 132.69, 132.76, 136.68, 136.20, 139.07, 139.83, 162.76.

4.1.1.6. (*E*)-9-(4-Fluorobenzylidene)-5-(4-fluorophenyl)-3-phenyl-6,7,8,9-tetrahydro-5*H*-pyrido[4,3-*d*]thiazolo[3,2-*a*]pyrimidine (6f). Yellow solid; yield: 85%, mp 161–164 °C; Anal. Calcd for $C_{28}H_{21}F_2N_3S$: C, 71.62; H, 4.51; N, 8.95; Found: C, 71.72; H, 4.57; N, 8.97; ^{1}H NMR (500 MHz, $CDCl_3$): δ_H 2.06 (br s, 1H, NH), 3.47 (d, J = 16.45 Hz, 1H, H-6a), 3.58 (d, J = 16.45 Hz, 1H, H-6b), 3.85 (d, J = 14.16 Hz, 1H, H-8a), 3.96 (d, J = 14.16 Hz, 1H, H-8b), 5.57 (s, 1H, H-5), 6.04 (s, 1H, H-2), 6.63–7.76 (m, 14H, H-aromatic, H-12). ^{13}C NMR (125 MHz, $CDCl_3$): δ_C 52.91, 53.49, 60.64, 101.45, 108.98, 125.07, 128.24, 128.53, 128.65, 128.90, 129.25, 129.71, 131.21, 131.32, 130.96, 133.78, 135.92, 139.35, 162.78.

4.1.1.7. (*E*)-9-(Benzylidene)-5-phenyl-3-(4-fluorophenyl)-6,7,8,9-tetrahydro-5*H*-pyrido[4,3-*d*]thiazolo[3,2-*a*]pyrimidine (6g). Yellow solid; yield: 81%, mp 192–194 °C; Anal. Calcd for $C_{28}H_{22}FN_3S$: C, 74.48; H, 4.91; N, 9.31; Found: C, 73.22; H, 4.31; N, 8.94; ^{1}H NMR (500 MHz, $CDCl_3$): δ_H 2.14 (br s, 1H, NH), 3.08 (d, J = 17.37 Hz, 1H, H-6a), 3.30 (d, J = 17.37 Hz, 1H, H-6b), 3.81 (d, J = 16.61 Hz, 1H, H-8a), 3.93 (d, J = 16.61 Hz, 1H, H-8b), 5.38 (s, 1H, H-5), 5.93 (s, 1H, H-2), 6.74–7.56 (m, 15H, H-aromatic, H-12). ^{13}C NMR (125 MHz, $CDCl_3$): δ_C 46.47, 46.73, 52.98, 53.79, 61.68, 111.84, 115.70, 115.99, 124.31, 126.68, 127.03, 128.47, 129.02, 131.04, 131.19, 132.43, 134.47, 137.87, 138.21, 141.45, 161.79, 165.10, 195.44.

4.1.1.8. (*E*)-9-(2-Chlorobenzylidene)-5-(2-chlorophenyl)-3-(4-fluorophenyl)-6,7,8,9-tetrahydro-5*H*-pyrido[4,3-*d*]thiazolo[3,2-*a*]pyrimidine (6h). Yellow solid; yield: 73%, mp 177–179 °C; Anal. Calcd for $C_{28}H_{20}Cl_2FN_3S$: C, 64.62; H, 3.87; N, 8.07; Found: C, 64.15; H, 3.59; N, 7.87; ^{1}H NMR (500 MHz, $CDCl_3$): δ_H 2.11 (br s, 1H, NH), 2.94 (d, J = 16.85 Hz, 1H, H-6a), 3.43 (d, J = 16.85 Hz, 1H, H-6b), 3.69 (d, J = 16.85 Hz, 1H, H-8a), 3.77 (d, J = 16.85 Hz, 1H, H-8b), 5.91 (s, 1H, H-5), 5.99 (s, 1H, H-2), 6.90–7.85 (m, 13H, H-aromatic, H-12). ^{13}C NMR (125 MHz, $CDCl_3$): δ_C 52.40, 52.81, 61.81, 100.40, 115.40, 115.56, 123.09, 126.03, 126.21, 127.95, 128.06, 128.91, 129.30, 129.37, 130.64, 130.68, 130.76, 130.87, 130.94, 131.82, 132.25, 133.68, 134.03, 135.85, 137.61, 138.90, 162.25, 162.47, 164.24, 164.67, 166.69, 195.01.

4.1.1.9. (*E*)-9-(2-Methoxybenzylidene)-5-(2-methoxyphenyl)-3-(4-fluorophenyl)-6,7,8,9-tetrahydro-5*H*-pyrido[4,3-*d*]thiazolo[3,2-*a*]pyrimidine (6i). Yellow solid; yield: 75%, mp 188–190 °C; Anal. Calcd for $C_{30}H_{26}FN_3O_2S$: C, 70.43; H, 5.12; N, 8.21; Found: C, 70.19; H, 4.88; N, 7.95; ^{1}H NMR (500 MHz, $CDCl_3$): δ_H 1.83 (br s, 1H, NH), 3.06 (d, J = 17.33 Hz, 1H, H-6a), 3.26 (d, J = 17.33 Hz, 1H, H-6b), 3.72 (s, 3H, O–CH_3), 3.80 (s, 3H, O–CH_3), 3.82 (d, J = 15.29 Hz, 1H, H-8a), 3.91 (d, J = 15.29 Hz, 1H, H-8b), 5.30 (s, 1H, H-5), 5.89 (s, 1H, H-2), 6.63–7.36 (m, 13H, H-aromatic, H-12). ^{13}C NMR (125 MHz, $CDCl_3$): δ_C 46.29, 46.42, 55.20, 55.22, 60.55, 100.22, 111.32, 113.59, 113.88, 115.37, 115.56, 123.22, 127.69, 130.62, 133.46, 134.12, 137.86, 158.27, 159.59, 161.93, 162.05, 164.03.

4.1.1.10. (*E*)-9-(4-Methylbenzylidene)-5-(4-methylphenyl)-3-(4-fuorophenyl)-6,7,8,9-tetrahydro-5*H*-pyrido[4,3-*d*]thiazolo[3,2-*a*]pyrimidine (6j). Yellow solid; yield: 79%, mp 119–121 °C; Anal. Calcd for $C_{30}H_{26}FN_3S$: C, 75.13; H, 5.46; N, 8.76; Found: C, 74.46; H, 5.19; N, 8.39; ^{1}H NMR (500 MHz, $CDCl_3$): δ_H 2.24 (s, 3H, CH_3), 2.35 (s, 3H, CH_3), 3.09 (d, J = 16.99 Hz, 1H, H-6a), 3.31 (d, J = 16.99 Hz, 1H, H-6b), 3.75 (d, J = 14.91 Hz, 1H, H-8a), 4.06 (d,

J = 14.91 Hz, 1H, H-8b), 5.42 (s, 1H, H-5), 5.93 (s, 1H, H-2), 6.57–7.52 (m, 13H, H-aromatic, H-12). ^{13}C NMR (125 MHz, $CDCl_3$): δ_C 21.47, 21.61, 45.23, 45.40, 61.36, 100.92, 109.05, 115.72, 116.00, 126.51, 129.47, 129.59, 129.75, 131.17, 131.28, 134.15, 134.22, 137.23, 134.22, 137.23, 138.22, 138.42, 138.76, 161.84, 162.92, 165.15.

4.1.1.11. (*E*)-9-(4-Chlorobenzylidene)-5-(4-chlorophenyl)-3-(4-fluorophenyl)-6,7,8,9-tetrahydro-5*H*-pyrido[4,3-*d*]thiazolo[3,2-*a*]pyrimidine (6k). Yellow solid; yield: 71%, mp 139-141 °C; Anal. Calcd for $C_{28}H_{20}Cl_2FN_3S$: C, 64.62; H, 3.87; N, 8.07; Found: C, 64.17; H, 3.44; N, 7.82; ^{1}H NMR (500 MHz, $CDCl_3$): δ_H 1.90 (s, 1H, NH), 3.05 (d, *J* = 17.00 Hz, 1H, H-6a), 3.29 (d, *J* = 17.00 Hz, 1H, H-6b), 3.78 (d, *J* = 15.00 Hz, 1H, H-8a), 3.89 (d, *J* = 15.00 Hz, 1H, H-8b), 5.37 (s, 1H, H-5), 5.96 (s, 1H, H-2), 6.61–7.83 (m, 13H, H-aromatic, H-12). ^{13}C NMR (125 MHz, $CDCl_3$): δ_C 45.92, 46.18, 60.53, 100.73, 115.58, 115.75, 123.13, 127.58, 127.66, 128.33, 128.78, 128.89, 130.55, 130.72, 134.22, 134.43, 135.78, 137.56, 139.46, 162.16.

4.1.1.12. (*E*)-9-(4-Fluorobenzylidene)-5-(4-fluorophenyl)-3-(4-fluorophenyl)-6,7,8,9-tetrahydro-5*H*-pyrido[4,3-*d*]thiazolo[3,2-*a*]pyrimidine (6l). Yellow solid; yield: 68%, mp 157–159 °C; Anal. Calcd for $C_{28}H_{20}F_3N_3S$: C, 68.98; H, 4.13; N, 8.62; Found: C, 68.54; H, 3.97; N, 8.25; ^{1}H NMR (500 MHz, $CDCl_3$): δ_H 3.20 (d, *J* = 16.70 Hz, 1H, H-6a), 3.39 (d, *J* = 16.70 Hz, 1H, H-6b), 3.80 (d, *J* = 14.97 Hz, 1H, H-8a), 3.90 (d, *J* = 14.97 Hz, 1H, H-8b), 5.48 (s, 1H, H-5), 5.97 (s, 1H, H-2), 6.67–7.26 (m, 13H, H-aromatic, H-12). ^{13}C NMR (125 MHz, $CDCl_3$): δ_C 52.64, 53.20, 60.39, 61.96, 101.97, 115.43, 115.60, 115.91, 128.08, 130.60, 130.68, 130.86, 137.73, 164.84, 194.75.

4.1.1.13. (*E*)-9-(Benzylidene)-5-phenyl-3-(4-chlorophenyl)-6,7,8,9-tetrahydro-5*H*-pyrido[4,3-*d*]thiazolo[3,2-*a*]pyrimidine (6m). Yellow solid; yield: 79%, mp 152–155 °C; Anal. Calcd for $C_{28}H_{22}ClN_3S$: C, 71.86; H, 4.74; N, 8.98; Found: C, 71.81; H, 4.749; N, 8.90; ^{1}H NMR (500 MHz, $CDCl_3$): δ_H 2.03 (br s, 1H, NH), 3.09 (d, *J* = 17.37 Hz, 1H, H-6a), 3.31 (d, *J* = 17.37 Hz, 1H, H-6b), 3.82 (d, *J* = 15.48 Hz, 1H, H-8a), 3.93 (d, *J* = 15.48 Hz, 1H, H-8b), 5.39 (s, 1H, H-5), 5.95 (s, 1H, H-2), 6.75–7.36 (m, 13H, H-aromatic), 7.45 (s, 1H, H-12). ^{13}C NMR (125 MHz, $CDCl_3$): δ_C 46.46, 46.72, 60.62, 101.12, 111.92, 124.34, 126.71, 126.93, 128.48, 128.84, 129.02, 129.06, 129.38, 129.75, 132.37, 134.51, 135.65, 137.83, 138.08, 141.26, 162.55.

4.1.1.14. (*E*)-9-(2-Chlorobenzylidene)-5-(2-chlorophenyl)-3-(4-chlorophenyl)-6,7,8,9-tetrahydro-5*H*-pyrido[4,3-*d*]thiazolo[3,2-*a*]pyrimidine (6n). Yellow solid; yield: 82%, mp 182–185 °C; Anal. Calcd for $C_{28}H_{20}Cl_3N_3S$: C, 62.64; H, 19.81; N, 7.83; Found: C, 62.51; H, 19.72; N, 7.69; ^{1}H NMR (500 MHz, $CDCl_3$): δ_H 2.10 (br s, 1H, NH), 2.94 (d, *J* = 16.55 Hz, 1H, H-6a), 3.43 (d, *J* = 16.55 Hz, 1H, H-6b), 3.69 (d, *J* = 15.25 Hz, 1H, H-8a), 3.76 (d, *J* = 15.25 Hz, 1H, H-8b), 5.92 (s, 1H, H-5), 5.99 (s, 1H, H-2), 6.84–7.76 (m, 12H, H-aromatic, H-12). ^{13}C NMR (125 MHz, $CDCl_3$): δ_C 52.38, 52.81, 61.86, 100.58, 108.74, 123.15, 126.17, 128.09, 128.65, 128.71, 128.96, 129.27, 129.39, 129.49, 130.17, 130.63, 131.77, 133.68, 134.03, 134.10, 135.53, 135.82, 137.48, 139.53, 162.47.

4.1.1.15. (*E*)-9-(2-Methoxybenzylidene)-5-(2-methoxyphenyl)-3-(4-chlorophenyl)-6,7,8,9-tetrahydro-5*H*-pyrido[4,3-*d*]thiazolo[3,2-*a*]pyrimidine (6o). Yellow solid; yield: 81%, mp 198–201 °C; Anal. Calcd for $C_{30}H_{26}ClN_3S$: C, 68.23; H, 4.96; N, 7.96; Found: C, 68.15; H, 4.75; N, 7.82; ^{1}H NMR (500 MHz, $CDCl_3$): δ_H 1.91 (br s, 1H, NH), 3.07 (d, *J* = 17.15 Hz, 1H, H-6a), 3.28 (d, *J* = 17.15 Hz, 1H, H-6b), 3.72 (s, 3H, O–CH_3), 3.81 (s, 3H, O–CH_3), 3.84 (d, *J* = 15.48 Hz, 1H, H-8a), 3.92 (d, *J* = 15.48 Hz, 1H, H-8b), 5.32 (s, 1H, H-5), 5.92 (s, 1H, H-2), 6.63–7.33 (m, 12H, H-aromatic), 7.37 (s, 1H, H-12). ^{13}C NMR (125 MHz, $CDCl_3$): δ_C 46.16, 46.29, 55.24, 60.52, 100.65, 111.11,123.46, 127.72, 128.66, 129.92, 130.08, 130.44, 132.62, 133.25, 134.22, 135.22, 137.77, 158.33, 159.65, 161.99.

4.1.1.16. (*E*)-9-(4-Methylbenzylidene)-5-(4-methylphenyl)-3-(4-chlorophenyl)-6,7,8,9-tetrahydro-5*H*-pyrido[4,3-*d*]thiazolo[3,2-*a*]pyrimidine (6p). Yellow solid; yield: 83%, mp 124–127 °C; Anal. Calcd for $C_{30}H_{26}ClN_3O_2S$: C, 72.64; H, 5.28; N, 8.47; Found: C, 72.61; H, 5.12; N, 8.32; ^{1}H NMR (500 MHz, $CDCl_3$): δ_H 2.21 (s, 3H, CH_3), 2.31 (s, 3H, CH_3), 3.24 (d, *J* = 17.05 Hz, 1H, H-6a), 3.60 (d, *J* = 17.05 Hz, 1H, H-6b), 3.84 (d, *J* = 15.10 Hz, 1H, H-8a), 4.01 (d, *J* = 15.10 Hz, 1H, H-8b), 5.47 (s, 1H, H-5), 5.96 (s, 1H, H-2), 6.56–7.36 (m, 12H, H-aromatic), 7.56 (s, 1H, H-12). ^{13}C NMR (125 MHz, $CDCl_3$): δ_C 21.04, 21.08, 43.94, 44.07, 60.71, 101.80, 117.88, 125.23, 126.15, 128.67, 129.01, 129.17, 129.21, 129.70, 130.14, 130.18, 133.27, 133.75, 135.37, 137.25, 138.61, 162.97.

4.1.1.17. (*E*)-9-(4-Chlorobenzylidene)-3,5-bis(4-chlorophenyl)-6,7,8,9-tetrahydro-5*H*-pyrido[4,3-*d*]thiazolo[3,2-*a*]pyrimidine (6q). Yellow solid; yield: 85%, mp 148–150 °C; Anal. Calcd for $C_{28}H_{20}Cl_3N_3S$: C, 62.64; H, 3.75; N, 7.83; Found: C, 62.55; H, 3.62; N, 7.81; ^{1}H NMR (500 MHz, $CDCl_3$): δ_H 1.94 (br s, 1H, NH), 3.05 (d, *J* = 17.40 Hz, 1H, H-6a), 3.28 (d, *J* = 17.40 Hz, 1H, H-6b), 3.77 (d, *J* = 15.29 Hz, 1H, H-8a), 3.87 (d, *J* = 15.29 Hz, 1H, H-8b), 5.36 (s, 1H, H-5), 5.96 (s, 1H, H-2), 6.66–7.34 (m, 12H, H-aromatic), 7.37 (s, 1H, H-12). ^{13}C NMR (125 MHz, $CDCl_3$): δ_C 46.04, 46.31, 60.46, 101.09, 111.43, 122.92, 127.71, 128.32, 128.76, 128.83, 128.93, 129.92, 130.57, 132.37, 132.47, 134.36, 134.47, 135.51, 135.84, 137.44, 139.33, 162.05.

4.1.1.18. (*E*)-9-(4-Fluorobenzylidene)-5-(4-fluorophenyl)-3-(4-chlorophenyl)-6,7,8,9-tetrahydro-5*H*-pyrido[4,3-*d*]thiazolo[3,2-*a*]pyrimidine (6r). Yellow solid; yield: 78%, mp 160–163 °C; Anal. Calcd for $C_{28}H_{20}ClF_2N_3S$: C, 66.73; H, 4.00; N, 8.34; Found: C, 66.65; H, 4.01; N, 8.12; ^{1}H NMR (500 MHz, $CDCl_3$): δ_H 2.14 (br s, 1H, NH), 3.06 (d, *J* = 17.20 Hz, 1H, H-6a), 3.32 (d, *J* = 17.20 Hz, 1H, H-6b), 3.62 (d, *J* = 15.65 Hz, 1H, H-8a), 3.86 (d, *J* = 15.65 Hz, 1H, H-8b), 5.39 (s, 1H, H-5), 5.97 (s, 1H, H-2), 6.64-7.47 (m, 12H, H-aromatic), 7.70 (s, 1H, H-12). ^{13}C NMR (125 MHz, $CDCl_3$): δ_C 52.52, 53.11, 60.50, 101.03, 108.46, 124.34, 128.03, 128.10, 128.72, 128.79, 129.49, 129.91, 129.94, 130.79, 130.85, 130.91, 133.92, 135.38, 136.67, 137.53, 139.64, 162.18.

4.1.1.19. (*E*)-9-(Benzylidene)-5-phenyl-3-(4-methoxyphenyl)-6,7,8,9-tetrahydro-5*H*-pyrido[4,3-*d*]thiazolo[3,2-*a*]pyrimidine (6s). Yellow solid; yield: 80%, mp 145–147 °C; Anal. Calcd for $C_{29}H_{25}N_3OS$: C, 75.13; H, 5.44; N, 9.06; Found: C, 74.22; H, 5.09; N, 9.21; ^{1}H NMR (500 MHz, $CDCl_3$): δ_H 2.54 (br s, 1H, NH), 3.10 (d, *J* = 17.28 Hz, 1H, H-6a), 3.32 (d, *J* = 17.28 Hz, 1H, H-6b), 3.81 (d, *J* = 15.12 Hz, 1H, H-8a), 3.84 (s, 3H, methoxy), 3.95 (d, *J* = 15.12 Hz, 1H, H-8b), 5.42 (s, 1H, H-5), 5.89 (s, 1H, H-2), 6.74-7.47 (m, 13H, H-aromatic), 7.54 (s, 1H, H-12). ^{13}C NMR (125 MHz, $CDCl_3$): δ_C 46.26, 46.55, 55.77, 61.42, 99.89, 111.47, 114.14, 123.25, 124.50, 126.77, 126.93, 128.49, 128.67, 128.93, 129.74, 130.55, 132.06, 134.55, 137.81, 139.07, 141.52, 160.58, 162.93.

4.1.1.20. (*E*)-9-(2-Chlorobenzylidene)-5-(2-chlorophenyl)-3-(4-methoxyphenyl)-6,7,8,9-tetrahydro-5*H*-pyrido[4,3-*d*]thiazolo[3,2-*a*]pyrimidine (6t). Yellow solid; yield: 76%, mp 172–174 °C; Anal. Calcd for $C_{29}H_{23}Cl_2N_3OS$: C, 65.41; H, 4.35; N, 7.89; Found: C, 65.12; H, 4.12; N, 8.17 ^{1}H NMR (500 MHz, $CDCl_3$): δ_H 2.59 (br s, 1H, NH), 3.28 (d, *J* = 16.45 Hz, 1H, H-6a), 3.64 (d, *J* = 16.45 Hz, 1H, H-6b), 3.69 (s, 3H, methoxy), 3.78 (s, 3H, methoxy), 3.83 (s, 3H, methoxy) 3.86 (d, *J* = 15.92 Hz, 1H, H-8a), 4.30

(d, J = 15.92 Hz, 1H, H-8b), 5.51 (s, 1H, H-5), 5.94 (s, 1H, H-2), 6.58-7.27 (m, 11H, H-aromatic), 7.61 (s, 1H, H-12). ^{13}C NMR (125 MHz, $CDCl_3$): δ_C 43.59, 55.23, 55.26, 55.41, 60.29, 100.38, 113.89, 114.05, 114.16, 114.33, 122.39, 126.78, 127.68, 128.16, 128.46, 130.37, 130.70, 132.57, 138.93, 159.03, 159.77, 160.35, 163.17.

4.1.1.21. (*E*)-9-(2-Methoxyphenylbenzylidene)-5-(2-methoxylphenyl)-3-(4-methoxyphenyl)-6,7,8,9-tetrahydro-5*H*-pyrido[4,3-*d*]thiazolo[3,2-*a*]pyrimidine (6u). Yellow solid; yield: 79%, mp 132–135 °C; Anal. Calcd for $C_{31}H_{29}N_3O_3S$: C, 71.10; H, 5.58; N, 8.02; Found: C, 71.54; H, 6.17; N, 8.72; ^{1}H NMR (500 MHz, $CDCl_3$): δ_H 2.49 (br s, 1H, NH), 3.46 (d, J = 17.49 Hz, 1H, H-6a), 3.54 (d, J = 17.49 Hz, 1H, H-6b), 3.72 (d, J = 16.07 Hz, 1H, H-8a), 3.80 (s, 3H, methoxy), 3.86 (d, J = 16.07 Hz, 1H, H-8b), 5.61 (s, 1H, H-5), 5.97 (s, 1H, H-2), 6.75-7.36 (m, 11H, H-aromatic), 7.69 (s, 1H, H-12). ^{13}C NMR (125 MHz, $CDCl_3$): δ_C 46.72, 46.93, 55.79, 61.56, 101.22, 111.52, 114.23, 123.39, 124.57, 126.82, 127.12, 128.54, 128.75, 129.11, 129.78, 130.69, 132.17, 134.63, 137.92, 139.18, 141.62, 160.71, 162.97.

4.1.1.22. (*E*)-9-(4-Methylbenzylidene)-5-(4-methylphenyl)-3-(4-methoxyphenyl)-6,7,8,9-tetrahydro-5*H*-pyrido[4,3-*d*]thiazolo[3,2-*a*]pyrimidine(6v). Yellow solid; yield: 84%, mp 158–161 °C; Anal. Calcd for $C_{31}H_{29}N_3OS$: C, 75.73; H, 5.95; N, 8.55; Found: C, 76.49; H, 6.64; N, 9.05; ^{1}H NMR (500 MHz, $CDCl_3$): δ_H 2.24 (s, 3H, CH_3), 2.35 (s, 3H, CH_3), 3.11 (d, J = 16.99 Hz, 1H, H-6a), 3.32 (d, J = 16.99 Hz, 1H, H-6b), 3.79 (d, J = 14.73 Hz, 1H, H-8a), 3.86 (s, 3H, methoxy), 4.02 (d, J = 14.73 Hz, 1H, H-8b), 5.41 (s, 1H, H-5), 5.89 (s, 1H, H-2), 6.58–7.14 (m, 11H, H-aromatic), 7.51 (s, 1H, H-12). ^{13}C NMR (125 MHz, $CDCl_3$): δ_C 21.55, 21.62, 45.50, 45.68, 55.79, 61.07, 100.01, 109.67, 114.17, 123.22, 125.53, 126.65, 129.40, 129.68, 130.62, 134.45, 137.05, 138.39, 138.58, 139.20, 160.60, 163.15.

4.1.1.23. (*E*)-9-(4-Chlorobenzylidene)-5-(4-chlorophenyl)-3-(4-methoxyphenyl)-6,7,8,9-tetrahydro-5*H*-pyrido[4,3-*d*]thiazolo[3,2-*a*]pyrimidine(6w). Yellow solid; yield: 87%, mp 169–171 °C; Anal. Calcd for $C_{29}H_{23}Cl_2N_3OS$: C, 65.41; H, 4.35; N, 7.89; Found: C, 65.12; H, 4.71; N, 8.21; ^{1}H NMR (500 MHz, $CDCl_3$): δ_H 2.41 (br s, 1H, NH), 3.39 (d, J = 16.65 Hz, 1H, H-6a), 3.67 (d, J = 16.65 Hz, 1H, H-6b), 3.77 (d, J = 14.65 Hz, 1H, H-8a), 3.85 (s, 3H, methoxy), 4.29 (d, J = 14.65 Hz, 1H, H-8b), 5.60 (s, 1H, H-5), 5.99 (s, 1H, H-2), 6.60–7.29 (m, 11H, H-aromatic), 7.58 (s, 1H, H-12). ^{13}C NMR (125 MHz, $CDCl_3$): δ_C 43.57, 55.12, 55.32, 55.67, 60.31, 100.07, 113.87, 114.17, 114.25, 114.33, 122.51, 126.79, 127.82, 128.22, 128.54, 130.49, 130.71, 132.62, 140.11, 159.27, 159.85, 160.19, 163.24.

4.1.1.24. (*E*)-9-(4-Fluorobenzylidene)-5-(4-fluorophenyl)-3-(4-methoxyphenyl)-6,7,8,9-tetrahydro-5*H*-pyrido[4,3-*d*]thiazolo[3,2-*a*]pyrimidine (6x). Yellow solid; yield: 83%, mp 212–215 °C; Anal. Calcd for $C_{29}H_{23}F_2N_3OS$: C, 69.72; H, 4.64; N, 8.41; Found: C, 70.72; H, 4.19; N, 8.21; ^{1}H NMR (500 MHz, $CDCl_3$): δ_H 2.05 (br s, 1H, NH), 3.05 (d, J = 17.35 Hz, 1H, H-6a), 3.28 (d, J = 17.35 Hz, 1H, H-6b), 3.35 (d, J = 16.20 Hz, 1H, H-8a), 3.71 (d, J = 14.20 Hz, 1H, H-6b), 3.85 (s, 3H, methoxy), 5.40 (s, 1H, H-5), 5.89 (s, 1H, H-2), 6.67–7.47 (m, 11H, H-aromatic), 7.80 (s, 1H, H-12). ^{13}C NMR (125 MHz, $CDCl_3$): δ_C 46.10, 52.65, 55.40, 60.24, 99.63, 108.59, 113.61, 113.84, 114.93, 115.10, 115.43, 122.74, 124.05, 128.12, 130.09, 130.30, 130.84, 132.04, 135.55, 134.33, 137.05, 138.52, 160.29, 163.58.

4.2. In vitro cholinesterase enzymes inhibitory assay

Cholinesterase enzymes inhibitory activity was evaluated using modified Ellman's method as described by Ahmed and Gilani.[41] Galanthamine was used as reference standard. Solutions of test samples and galanthamine were prepared in DMSO at an initial concentration of 1 mg/mL (1000 ppm). The concentration of DMSO in final reaction mixture was 1%. At this concentration, DMSO has no inhibitory effect on both AChE and BChE enzymes.[42]

For acetylcholinesterase (AChE) inhibitory assay, 140 μL of 0.1 M sodium phosphate buffer of pH 8 was first added to a 96-wells microplate followed by 20 μL of test samples and 20 μL of 0.09 units/mL acetylcholinesterase. After 15 min of incubation at 25 °C, 10 μL of 10 mM 5,5′-dithiobis-2-nitrobenzoic acid (DTNB) was added into each well followed by 10 μL of 14 mM acetylthiocholine iodide. Absorbance of the colored end-product was measured using BioTek PowerWave X 340 Microplate Spectrophotometer at 412 nm for 30 min after the initiation of enzymatic reaction. For butyrylcholinesterase (BChE) inhibitory assay, the same procedure described above was followed, except for the use of enzyme and substrate, instead of which, butyrylcholine esterase from equine serum and *S*-butyrylthiocholine chloride were used.

Each test was conducted in triplicate. Absorbance of the test samples was corrected by subtracting the absorbance of their respective blank. Percentage inhibition was calculated using the following formula:

$$\text{Percentage of inhibition} = \frac{\text{Absorbance of control} - \text{Absorbance of Sample}}{\text{Absorbance of control}} \times 100.$$

4.3. Molecular docking studies

Using Glide™, (version 5.7, Schrödinger, LLC, New York, NY, 2011), the most active compound, **6d**, were docked onto the active site of *h*AChE derived from the crystal structures of the enzyme complexed with the anti-Alzheimer's drug, galanthamine (PDB ID: 4EY6) and to *h*BChE derived from the crystal structure of the complex of the enzyme with its substrate BCh (PDB code: 1P0P).

Water molecules and hetero groups were deleted from the enzyme beyond the radius of 5 Å of the reference ligand (galanthamine or BCh), and the resulting protein structure refined and minimized by Protein Preparation Wizard™ using the OPLS-2005 force field. The Receptor Grid Generation program was used to prepare *h*AChE and *h*BChE grid and all the ligands were optimized by LigPrep™ using the OPLS-2005 force field to generate the lowest energy state of the respective ligands. Docking stimulations were carried out on bioactive compounds to generate 5 poses per ligand, and the best pose (with the highest score) displayed for each.

Acknowledgments

We would like to thank the Malaysian Government and Universiti Sains Malaysia (USM) for the Research University Grant (1001/PFARMASI/813031). A.B. is supported by the USM Graduate Assistant Scheme from the Institute for Postgraduate Studies (IPS) of Universiti Sains Malaysia.

Supplementary data

Supplementary data associated with this article can be found, in the online version, at http://dx.doi.org/10.1016/j.bmc.2013.11.020.

References and notes

1. Yi, F.; Peng, Y.; Song, G. *Tetrahedron Lett.* **2005**, *46*, 3931.
2. Dandia, A.; Jain, A. K.; Laxkar, A. K.; Bhati, D. S. *Tetrahedron* **2013**, *69*, 2062.

3. Al-Omary, F. A.; Hassan, G. S.; El-Messery, S. M.; El-Subbagh, H. I. *Eur. J. Med. Chem.* **2012**, *47*, 65.
4. El-Nassan, H. B. *Eur. J. Med. Chem.* **2013**, *62*, 614.
5. Svetlik, J.; Veizerová, L.; Mayer, T. U.; Catarinella, M. *Bioorg. Med. Chem. Lett.* **2010**, *20*, 4073.
6. Hu, J.; Wang, Y.; Wei, X.; Wu, X.; Chen, G.; Cao, G.; Shen, X.; Zhang, X.; Tang, Q.; Liang, G. *Eur. J. Med. Chem.* **2013**, *64*, 292.
7. Luthra, P. M.; Mishra, C. B.; Jha, P. K.; Barodia, S. K. *Bioorg. Med. Chem. Lett.* **2010**, *20*, 1214.
8. Abdel-Hafez, A. A.; El-Sherief, H. A.; Jo, M.; Kurokawa, M.; Shiraki, K.; Kawahata, T.; Otake, T.; Nakamura, N.; Hattori, M. *Arzneim.-Forsch.* **2002**, *52*, 833.
9. Fatima, S.; Sharma, A.; Saxena, R.; Tripathi, R.; Shukla, S. K.; Pandey, S. K.; Tripathi, R.; Tripathi, R. P. *Eur. J. Med. Chem.* **2012**, *55*, 195.
10. Zhi, H.; Chen, L.; Zhang, L.; Liu, S.; Wan, D. C. C.; Lin, H.; Hu, C. *Arkivoc* **2008**, *13*, 266.
11. Mohamed, T.; Rao, P. P. *Bioorg. Med. Chem. Lett.* **2010**, *20*, 3606.
12. Mohamed, T.; Zhao, X.; Habib, L. K.; Yang, J.; Rao, P. P. *Bioorg. Med. Chem.* **2011**, *19*, 2269.
13. Mohamed, T.; Yeung, J. C. K.; Vasefi, M. S.; Beazely, M. A.; Rao, P. P. N. *Bioorg. Med. Chem. Lett.* **2012**, *22*, 4707.
14. Mohamed, T.; Yeung, J. C.; Rao, P. P. *Bioorg. Med. Chem. Lett.* **2011**, *21*, 5881.
15. Figueiredo, J.; Ismael, M.; Pinheiro, J.; Silva, A.; Justino, J.; Silva, F.; Goulart, M.; Mira, D.; Araújo, M.; Campoy, R. *Carbohydrate Res.* **2012**, *347*, 47.
16. Basiri, A.; Murugaiyah, V.; Osman, H.; Kumar, R. S.; Kia, Y.; Ali, M. A. *Bioorg. Med. Chem.* **2013**, *67*, 221.
17. Mount, C.; Downton, C. *Nat. Med.* **2006**, *12*, 780.
18. Terry, R. D.; Gonatas, N. K.; Weiss, M. *Annu. J. Pathol* **1964**, *44*, 269.
19. Perry, E. K.; Tomlinson, B. E.; Blesseed, G.; Bergmann, K.; Gibson, P. H.; Perry, R. H. *Br. Med. J.* **1978**, *2*, 1457.
20. Klafki, H. W.; Staufenbiel, M.; Kornhuber, J.; Wiltfang, J. *Brain* **2006**, *129*, 2840.
21. Grundke-Iqbal, I.; Iqbal, K.; Tung, Y. C.; Quinlan, M.; Wisniewski, H. M.; Binder, L. *Proc. Natl. Acad. Sci. U.S.A.* **1989**, *86*, 2853.
22. Coyle, J. T.; Puttfarcken, P. *Science* **1993**, *262*, 689.
23. Goedert, M.; Spillantini, M. G. A. *Science* **2006**, *314*, 777.
24. Farlow, M.; Miller, M.; Pejovic, V. *Dement. Geriatr. Cogn. Disord.* **2008**, *25*, 408.
25. Gianni, B.; Antonio, M. *Eur. J. Pharm. Sci.* **1998**, *346*, 1.
26. Tabet, N. *Age Ageing* **2006**, *35*, 336.
27. Andreani, A.; Burnelli, S.; Granaiola, M.; Guardigli, M.; Leoni, A.; Locatelli, A.; Morigi, R.; Rambaldi, M.; Rizzoli, M.; Varoli, L.; Roda, A. *Eur. J. Med. Chem.* **2008**, *43*, 657.
28. Ballard, C. *Eur. Neurol.* **2002**, *47*, 64.
29. Giacobini, E. *Pharmacol. Res.* **2004**, *50*, 433.
30. Greig, N.; Utsuki, T.; Ingram, D.; Wang, Y.; Pepeu, G.; Scali, C.; Yu, Q.; Mamczarz, J.; Holloway, H.; Giordano, T.; Chen, D.; Furukawa, K.; Sambamurti, K.; Brossi, A.; Lahiri, D. *Proc. Natl. Acad. Sci. U.S.A.* **2005**, *102*, 17213.
31. Xie, W.; Stribley, J. A.; Chatonnet, A.; Wilder, P. J.; Rizzino, A.; McComb, R. D.; Taylor, P.; Hinrichs, S. H.; Lockridge, O. *J. Pharmacol. Exp. Ther.* **2000**, *293*, 896.
32. Sussman, J. L.; Harel, M.; Frolow, F.; Oefner, C.; Goldman, A.; Toker, L.; Silman, I. *Science* **1991**, *253*, 872.
33. Harel, M.; Quinn, D. M.; Nair, H. K.; Silman, I.; Sussman, J. L. *J. Am. Chem. Soc.* **1996**, *118*, 2340.
34. Harel, M.; Schalk, I.; Ehret-Sabatier, L.; Bouet, F.; Goeldner, M.; Hirth, C.; Axelsen, P. H.; Silman, I.; Sussman, J. L. *Proc. Natl. Acad. Sci. U.S.A.* **1993**, *90*, 9031.
35. Pezzementi, L.; Nachon, F.; Chatonnet, A. *PLoS One* **1932**, *2011*, 6.
36. Çokuğraş, A. N. *Turk. J. Biochem.* **2003**, *28*, 54.
37. Koellner, G.; Steiner, T.; Millard, C. B.; Silman, I.; Sussman, J. L. *J. Mol. Biol.* **2002**, *320*, 721.
38. Nicolet, Y.; Lockridge, O.; Masson, P.; Fontecilla-Camps, J. C.; Nachon, F. *J. Biol. Chem* **2003**, *278*, 41141.
39. Dimmock, J. R.; Padmanilayam, M. P.; Puthucode, R. N.; Nazarali, A. J.; Motaganahalli, N. L.; Zello, G. A.; Quail, J. W.; Oloo, E. O.; Kraatz, H. B.; Prisciak, J. S. *J. Med. Chem.* **2001**, *44*, 586.
40. Wong, K. K. K.; Ngo, J. C. K.; Liu, S.; Lin, H.; Hu, C.; Shaw, P. C.; Wan, D. C. C. *Chem.-Biol. Interact.* **2012**, *187*, 335.
41. Ahmed, T.; Gilani, A. H. *Pharmacol. Biochem. Behavior* **2009**, *91*, 554.
42. Obregon, A.; Schetinger, M.; Correa, M. M.; Morsch, V. M.; Da Silva, J.; Martins, M.; Bonacorso, H. G.; Zanatta, N. *Neurochem. Res.* **2005**, *30*, 379.